

See discussions, stats, and author profiles for this publication at: <https://www.researchgate.net/publication/14457957>

# Active site properties of monomeric triosephosphate isomerase (monoTIM) as deduced from mutational and structural studies

ARTICLE *in* PROTEIN SCIENCE · FEBRUARY 2008

Impact Factor: 2.85 · DOI: 10.1002/pro.5560050206 · Source: PubMed

---

CITATIONS

36

---

READS

17

## 4 AUTHORS, INCLUDING:



[Narmada Thanki](#)

National Institutes of Health

44 PUBLICATIONS 5,392 CITATIONS

[SEE PROFILE](#)



[Ramon Eritja](#)

Spanish National Research Council

375 PUBLICATIONS 7,025 CITATIONS

[SEE PROFILE](#)



[Rik Wierenga](#)

University of Oulu

207 PUBLICATIONS 8,571 CITATIONS

[SEE PROFILE](#)

# Active site properties of monomeric triosephosphate isomerase (monoTIM) as deduced from mutational and structural studies

WOLFGANG SCHLIEBS, NARMADA THANKI, RAMON ERITJA, AND RIK WIERENGA

European Molecular Biology Laboratory, Postfach 102209, D-69012 Heidelberg, Germany

(RECEIVED August 9, 1995; ACCEPTED November 20, 1995)

## Abstract

MonoTIM is a stable monomeric variant of the dimeric trypanosomal enzyme triose phosphate isomerase (TIM) with less, but significant, catalytic activity. It is known that in TIM, three residues, Lys 13 (loop 1), His 95 (loop 4), and Glu 167 (loop 6) are the crucial catalytic residues. In the wild-type TIM dimer, loop 1 and loop 4 are very rigid because of tight interactions with residues of the other subunit. Previous structural studies indicate that Lys 13 and His 95 have much increased conformational flexibility in monoTIM. Using site-directed mutagenesis, it is shown here that Lys 13 and His 95 are nevertheless essential for optimal catalysis by monoTIM: monoTIM-K13A is completely inactive, although it can still bind substrate analogues, and monoTIM-H95A is 50 times less active. The best inhibitors of wild-type TIM are phosphoglycolohydroxamate (PGH) and 2-phosphoglycolate (2PG), with  $K_i$  values of 8  $\mu\text{M}$  and 26  $\mu\text{M}$ , respectively. The affinity of the monoTIM active site for PGH has been reduced approximately 60-fold, whereas for 2PG, only a twofold weakening of affinity is observed. The mode of binding, as determined by protein crystallographic analysis of these substrate analogues, shows that, in particular, 2PG interacts with Lys 13 and His 95 in a way similar but not identical to that observed for the wild-type enzyme. This crystallographic analysis also shows that Glu 167 has the same interactions with the substrate analogues as in the wild type. The data presented suggest that, despite the absence of the second subunit, monoTIM catalyzes the interconversion of D-glyceraldehyde-3-phosphate and dihydroxyacetone phosphate via the same mechanism as in the wild type.

**Keywords:** active site; crystal structures; dimer interface; monoTIM; mutagenesis; TIM

Triose phosphate isomerase (TIM) is an essential glycolytic enzyme (Knowles, 1991), which catalyzes the interconversion of D-glyceraldehyde-3-phosphate (GAP) and dihydroxyacetone phosphate (DHAP) (Fig. 1). It is a very tight dimer (Borchert et al., 1994), consisting of two identical subunits of 250 residues. Only the intact dimer is fully active (Waley, 1973; Zabori et al., 1980). It has been shown that it is a very efficient enzyme, which in vivo catalyzes the interconversion at a rate limited only by diffusion (Knowles & Albery, 1977). The important catalytic residues are Lys 13, His 95, and Glu 167, when using the numbering scheme of trypanosomal TIM (Fig. 2).

Reprint requests to: R.K. Wierenga, EMBL, Postfach 102209, D-69012 Heidelberg, Germany; e-mail: wierenga@embl-heidelberg.de.

**Abbreviations:** DHAP: dihydroxyacetone phosphate, DTT: dithiothreitol (reduced form), EDTA: ethylenediaminetetraacetate, GAP: D-glyceraldehyde-3-phosphate, MOPS: 3-[N-morpholino]propane sulfonic acid, PGH: phosphoglycolohydroxamate, TEA: triethanolamine, TIM: triosephosphate isomerase, wtTIM: wild-type trypanosomal triosephosphate isomerase, 2PG: 2-phosphoglycolate.

The best competitive inhibitors of wild-type TIM are phosphoglycolohydroxamate (PGH) and 2-phosphoglycolate (2PG), with  $K_i$  values near 10  $\mu\text{M}$  (Wolfenden, 1969; Collins, 1974). Their covalent structures are depicted in Figure 3. Crystal structures of the complexes of TIM with 2PG (Lolis & Petsko, 1990) and PGH (Davenport et al., 1991; Noble et al., 1993) have been determined. The mode of binding of PGH with respect to the catalytic residues is shown in Figure 4. Detailed studies of the reaction mechanism have shown (Knowles, 1991) that, after substrate binding, the following steps can be recognized in the conversion of DHAP into GAP. (1) The unprotonated glutamate side chain of the catalytic glutamate (Glu 167 in trypanosomal TIM) abstracts a proton from C-9 (equivalent to N-9 in PGH), which generates an enediolate intermediate with the atoms C-7, O-8, C-9, and O-10 in one plane (as in PGH). (2) The histidine side chain of His 95 facilitates proton transfer between O-8 and O-10. (3) The protonated glutamate side chain delivers the proton back to C-7, which completes the two proton transfer steps.

As can be seen in Figure 4, in the PGH complex, the Glu 167 side chain is well positioned (above the plane) for proton trans-

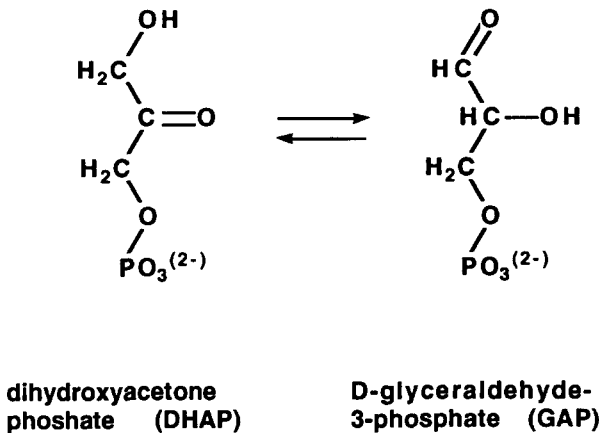


Fig. 1. Reaction catalyzed by TIM.

fer between the two carbon atoms, and  $N_{\epsilon}2$ (His 95) can facilitate the proton transfer between the O-8 and O-10 atoms. The positively charged atoms  $N_{\epsilon}$ (Lys 13) and  $N_{\delta}1$ (Asn 11), below the plane of the enediolate moiety, will facilitate the proton transfer by the catalytic glutamate. The mode of binding of the enediolate intermediate in the active site is such that the undesirable side reaction, which is a methylglyoxal synthase activity (Richard, 1984) that results in phosphate elimination and methylglyoxal formation, does not occur to any significant extent (Pompliano et al., 1990).

The TIM subunit has the  $(\beta\alpha)^8$  fold, with a central core of eight parallel  $\beta$  strands (strand 1 to strand 8) covered on the out-

side by eight  $\alpha$  helices (helix 1 to helix 8) (Figs. 2 and 4). The active site is formed by the loops following immediately after the  $\beta$  strands. These loops are numbered loop 1 to loop 8, in correspondence with the numbering of the preceding  $\beta$  strands. The catalytic residues are in loop 1 (Lys 13), loop 4 (His 95), and loop 6 (Glu 167). Loops 1–4 also form the dimer interface. Between loops 1 and 4 of the same subunit is a deep pocket, near the active site. There is only one interaction between loops 1 and 4 of the same subunit, which is the salt bridge between Lys 13 and Glu 97. In addition, in the unliganded structure, there is a water-mediated interaction between the side chains of Asn 11 (loop 1) and His 95 (loop 4) (Wierenga et al., 1992).

Two of the loops after the  $\beta$  strands protrude out of the bulk of the subunit: loop 3 and loop 6. Loop 3 of subunit 2 docks into the deep pocket between loop 1 and loop 4 of subunit 1; it interacts with Lys 13 and Glu 97 via van der Waals contacts and via a hydrogen bond between Thr 75 at the tip of loop 3 and the carboxylic acid moiety of Glu 97 (Fig. 5). The active site pocket is therefore close to the dimer interface, near to the docked loop 3 of the other subunit. However, the residues interacting directly with the substrate analogues are all from the same subunit. The shortest distance between Thr 75 at the tip of loop 3 of the other subunit and the ligand is approximately 5 Å. The second long loop, loop 6, protrudes into the solvent in the unliganded (open) form, and closes off the active site in the liganded (closed) form (Joseph et al., 1990, Williams & McDermott, 1995).

MonoTIM is a recombinant monomeric variant of wild-type trypanosomal TIM (wtTIM). It is made by replacing the 15 residues of the interface loop 3 by eight residues. The numbering scheme and sequence of wtTIM and monoTIM are shown in

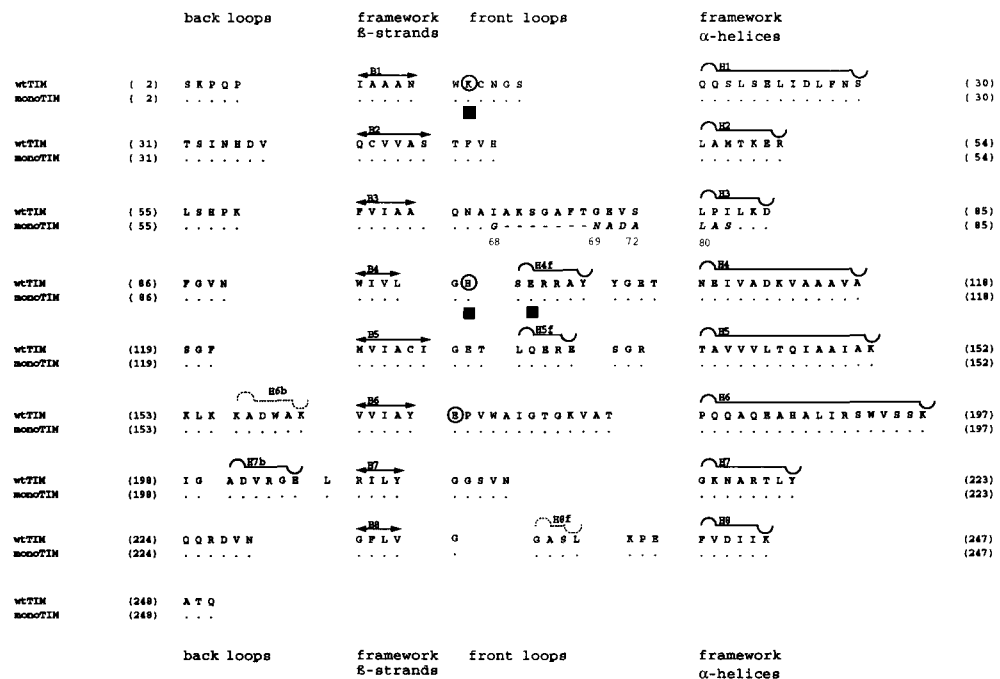
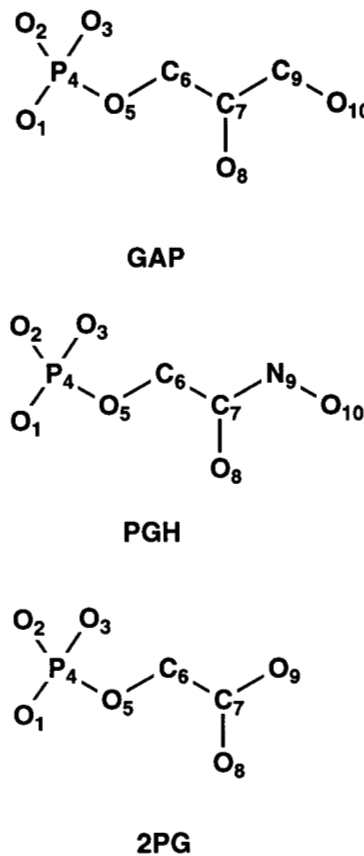


Fig. 2. Sequences of wtTIM and monoTIM. The  $\beta$  strands and  $\alpha$  helices of the wtTIM structure are indicated by solid lines;  $\beta_{10}$  helices are marked by dotted lines. MonoTIM has the same sequence as wtTIM except in front loop 3, where it is seven residues shorter (indicated by —). The adopted numbering scheme of monoTIM is discontinuous in this region, as indicated in the figure. The catalytic residues Lys 13, His 95, and Glu 167 are circled. Active site residues that have been mutated are indicated (■).



**Fig. 3.** Atom numbering scheme for GAP, PGH, and 2PG.

Figure 2. MonoTIM is a stable protein. Its catalytic activity is significant, but the  $k_{cat}$  is 1,000 times lower than that of the wild-type enzyme. The crystal structure of monoTIM showed that loop 1 and loop 4 had considerably different structural properties than in the wild type. Loop 1 (with Lys 13) was completely mobile (invisible in the electron density map), and loop 4 (with His 95) had adopted a very different conformation. Recently, three more crystal structures of point mutation variants of monoTIM have been described (Borchert et al., 1995). These structures showed that loop 1 and loop 4 can adopt different

structures, depending on experimental conditions such as crystal packing and the presence (or absence) of active site ligands. Most importantly, these new structures showed that Lys 13 in loop 1, His 95 in loop 4, and Glu 167 in loop 6 in monoTIM can adopt wild-type-like conformations in the presence of active site ligands.

In this paper, we further investigate the importance of Lys 13 and His 95 for the catalytic properties of monoTIM. For this purpose, point mutations have been made in monoTIM in loop 1 (Lys 13) and loop 4 (His 95 and Glu 97). Lys 13 has been changed into an arginine and alanine, and His 95 and Glu 97 into alanine. Catalytic properties of these variants have been determined. Also, the inhibitory properties of 2PG and PGH for monoTIM were determined. Mutagenesis experiments show that Lys 13 and His 95 are essential for optimal catalysis by mono-TIM, as in the wild type.

## Results

### Properties of monoTIM

Most of these studies have been done with monoTIM, but some (Table 1) have been done with monoTIM-SS (monoTIM with the mutations F45S, V46S) or monoTIM-W (monoTIM with the mutation A100W). MonoTIM-SS and monoTIM-W have essentially the same kinetic properties as monoTIM (Table 2), but they crystallize in different space groups (Borchert et al., 1995).

The catalytic constants for the interconversion of GAP and DHAP by monoTIM and wtTIM are compared in Table 2. The monoTIM  $k_{cat}$ 's for both reactions are at least 1,000-fold lower, and the monoTIM  $K_m$ 's for both substrates approximately 10-fold higher, than for the wild type, whereas the monoTIM  $K_I$ 's for 2PG are only two times higher than the corresponding wtTIM  $K_I$ , indicating that the affinities of monoTIM and wtTIM for 2PG are rather similar. However, the affinity of the monoTIM active site for PGH is almost 100-fold lower (Table 2).

The stability of monoTIM has been studied by temperature-dependent CD measurements. The change of the far-UV CD spectrum as a function of temperature is shown in Figure 6A for monoTIM-SS. The CD melting curves, measured at 222 nm, as shown in Figure 6B and C, show that the stabilities of wtTIM and monoTIM are very similar. Under the conditions tested, the  $T_m$  is approximately 52 °C in the absence of 2PG, whereas in the presence of 1 mM 2PG, the  $T_m$  is increased to 57 °C.

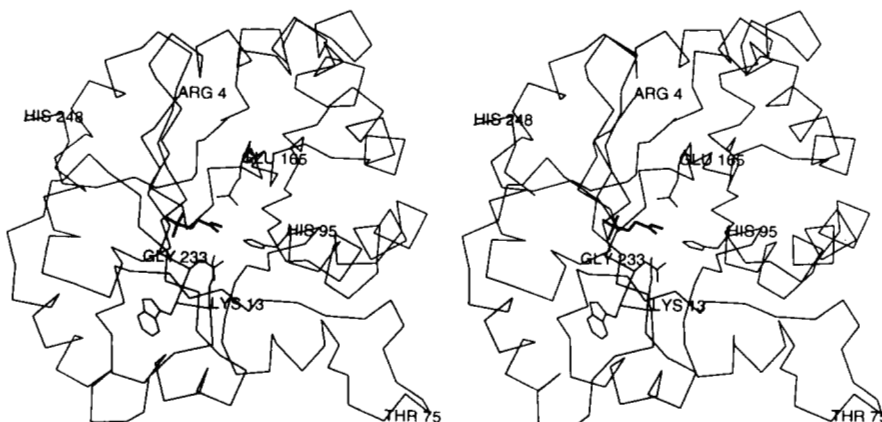


**Fig. 4.** PGH bound in the active site of wild-type chicken TIM. PGH is drawn in bold lines; the C $\alpha$  trace is drawn in thin lines (only one subunit is shown). The side chains of Asn 11-Trp 12-Lys 13 (loop 1), His 95 (loop 4), and Glu 165 (loop 6) are also shown. Glu 165 (chicken TIM) is equivalent to Glu 167 of trypanosomal TIM. Thr 75 marks the tip of loop 3, which is deleted in monoTIM. Arg 4 and His 249 label the N-terminus and C-terminus, respectively.

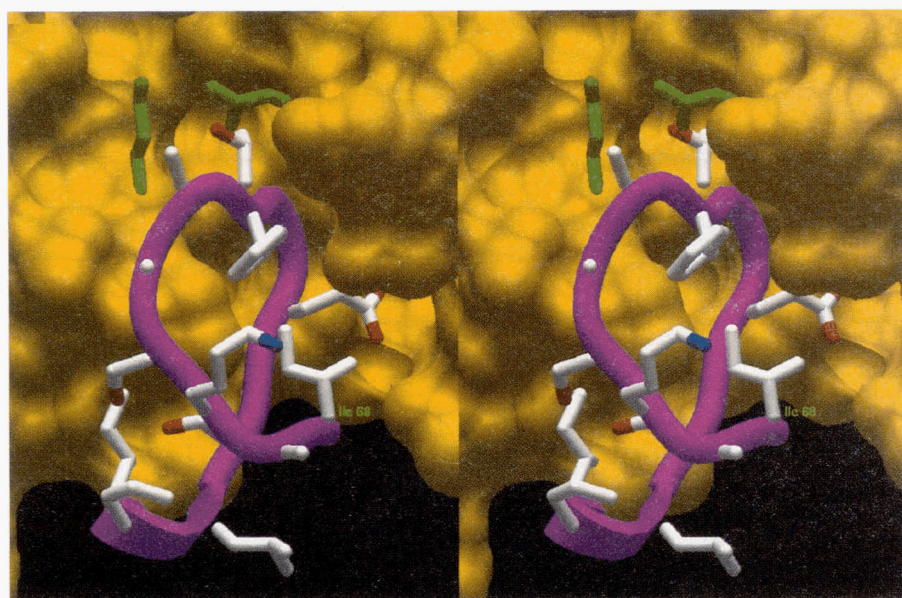


**Fig. 5.** Docking of loop 3 of subunit 2 into the pocket near the active site of subunit 1. The surface of subunit 1 (shown in yellow) is calculated excluding the side chains of Lys 13 and Glu 97. These side chains are explicitly shown in green. The sequence of the loop-3 fragment is Ile 68-Ala-Lys-Ser-Gly-Ala-Phe-Thr 75-Gly-Glu-Val-Ser-Leu-Pro-Ile 82. This loop-3 fragment circles around Cys 14 of subunit 1. Thr 75 of this loop is hydrogen bonded to the side chain of Glu 97 of the other subunit. This figure was prepared with ICM 2.0 (Biosoft, New York, USA) (Abagyan et al., 1994).

MonoTIM-SS and monoTIM-W have the same stability properties as monoTIM (data not shown).

For some variants of wild-type chicken TIM, an increased methylglyoxal synthase activity is observed (Blacklow & Knowles, 1990; Pompliano et al., 1990). The formation of methylglyoxal in the presence of monoTIM and GAP has been tested under standard assay conditions, without coupling enzyme, by taking aliquots of reaction mixture at different times and measuring the methylglyoxal concentration. No monoTIM-catalyzed formation of methylglyoxal could be detected.

#### Loop-1 point mutations

The variant monoTIM-K13R is still active, but its  $k_{cat}$  is 30 times lower, whereas  $K_m$  is unchanged (Table 3). The affinity of 2PG for monoTIM-K13R and monoTIM is similar, as can be deduced from the respective  $K_f$  values (Table 3). MonoTIM-K13A is inactive, but it can still bind 2PG, as is indicated by the shift of the CD melting curve to higher temperatures in the presence of 2PG (Fig. 6D). The  $T_m$  values for monoTIM-K13A in

the absence and presence of 1 mM 2PG are 52 °C and 57 °C, respectively, as also observed for monoTIM (Fig. 6C).

#### Loop-4 point mutations

Two active site residues of loop 4, His 95 and Glu 97, have been mutated into alanines. The H95A variant is approximately 50 times less active, and the  $K_m$  is unchanged (Table 3). The  $K_f$  of 2PG is increased more than sixfold, indicating a much reduced affinity of the active site of monoTIM-H95A for 2PG. The mutation E97A does not result in a significant change in the kinetic parameters (Table 3).

#### Mode of binding of PGH and 2PG in the active site of monoTIM

Table 4 lists the potential hydrogen bond interactions between polar protein and ligand atoms. In this table are also included the wild-type TIM data of the chicken TIM PGH complex and the yeast TIM 2PG complex. The conformational dihedral an-

**Table 1.** Different variants of monoTIM

Nomenclature	Mutations with respect to monoTIM	Reference	Crystallographic data	
			PDB entry	Active site ligand
monoTIM		Borchert et al., 1993a	1TRI	sulfate
monoTIM-SS	F45S, V46S	Borchert et al., 1995	1MSS	unliganded
monoTIM-SS	F45S, V46S	Borchert et al., 1995	1TTJ	PGH
monoTIM-W	A100W	Borchert et al., 1995	1TTI	2PG
monoTIM-W-E97A	A100W, E97A	This paper		
monoTIM-H95A	H95A	This paper		
monoTIM-K13R	K13R	This paper		
monoTIM-K13A	K13A	This paper		

**Table 2.** Steady-state kinetic data for wtTIM and monoTIM<sup>a</sup>

Protein	$k_{cat}^b$ (min <sup>-1</sup> )	$k_{cat}^c$ (min <sup>-1</sup> )	$K_m^b$ (mM)	$K_m^c$ (mM)	$K_I$ (2PG) <sup>b</sup> (μM)	$K_I$ (PGH) <sup>b</sup> (mM)
wtTIM	$3.7 \times 10^{5d}$	$6.5 \times 10^{4d}$	$0.25 \pm 0.05^d$	$1.2 \pm 0.1^d$	$26 \pm 7$	$0.008 \pm 0.001$
monoTIM	$3.1 \times 10^2$	12	$4.1 \pm 0.6$	$12.2 \pm 1.9$	$52 \pm 7$	$0.50 \pm 0.1$
monoTIM-SS	$4.7 \times 10^2$	40.6	$6.1 \pm 0.5$	$18 \pm 3.5$	$73 \pm 5$	$0.55 \pm 0.1$
monoTIM-W	$2.6 \times 10^2$	37.7	$3.1 \pm 1.3$	$17.6 \pm 2.2$	$51 \pm 7$	$0.61 \pm 0.1$

<sup>a</sup> The  $K_I$ 's have been calculated with GraFit, assuming competitive inhibition.<sup>b</sup> With GAP as substrate.<sup>c</sup> With DHAP as substrate.<sup>d</sup> As reported previously (Lambeir et al., 1987).

gles of 2PG and PGH bound to monoTIM and wtTIM are different (Table 5, Fig. 7). Nevertheless, the data of Table 4 show that the protein-ligand interactions in the monoTIM(2PG) complex and in the yeast TIM(2PG) complex are essentially the same. This is so for the phosphate moiety as well as for the interactions of the carboxylic acid atoms O-8 and O-9. In both complexes,

the carboxylate atom O-9(2PG) interacts with N<sub>ε</sub>2(His 95), O<sub>ε</sub>1(Glu 167) and O<sub>ε</sub>2(Glu 167), whereas O-8(2PG) interacts with N<sub>δ</sub>2(Asn 11), N<sub>ε</sub>2(His 95), and N<sub>ζ</sub>(Lys 13). Nevertheless, in monoTIM, the O-8(2PG) [as well as the N<sub>ζ</sub>(Lys 13) atom] has moved away from the active site pocket owing to differences in the dihedrals  $\chi$ <sub>a</sub> and  $\chi$ <sub>c</sub> (Table 5). Compared to the wild type,

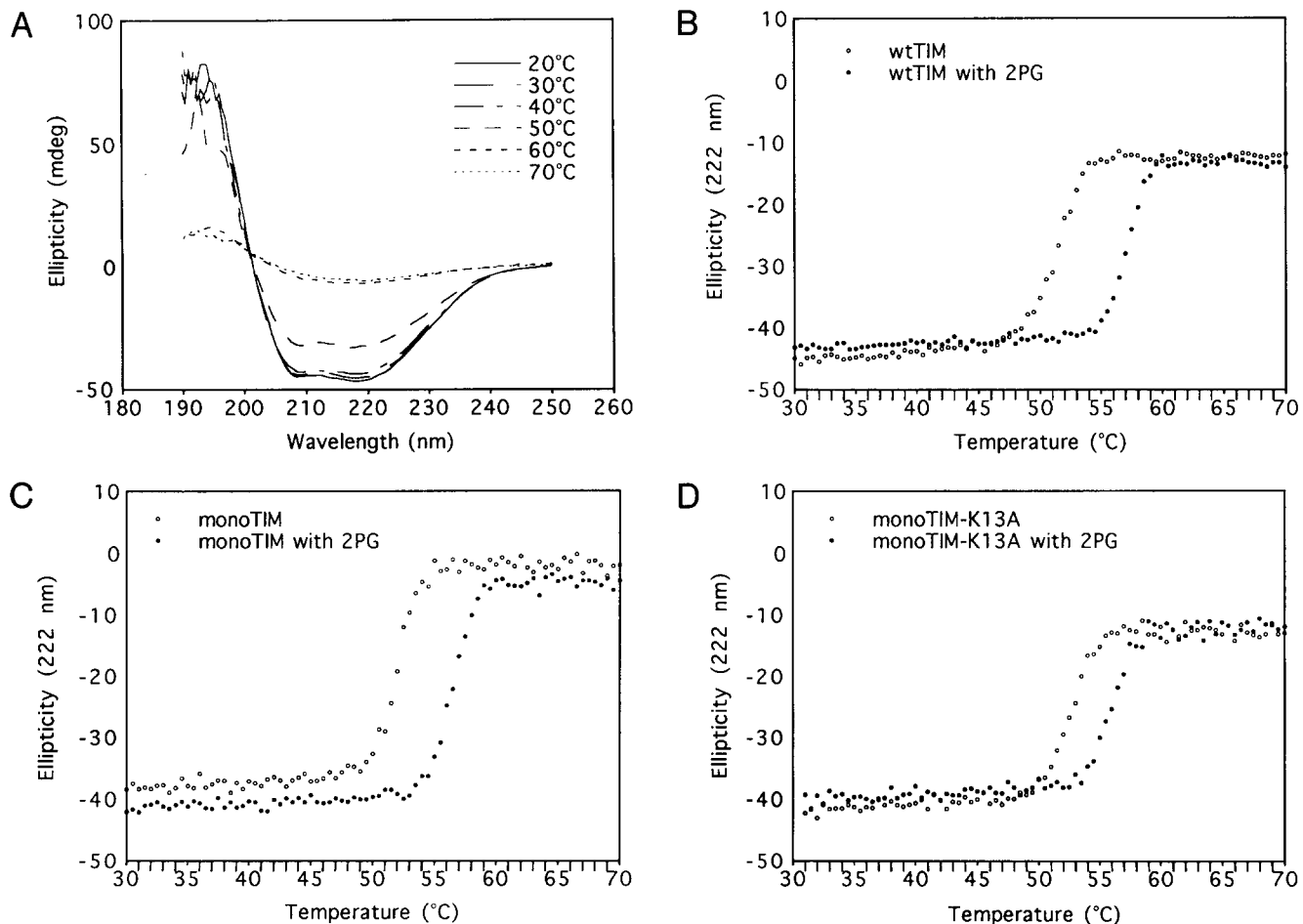


**Fig. 6.** Thermal stability of monoTIM. **A:** Typical far-UV CD spectra of the monoTIM variants recorded at different temperatures, as measured with monoTIM-SS (0.5 mg/mL) in 20 mM phosphate buffer, pH = 7.0. **B,C,D:** Thermal denaturation curves of wtTIM (B), monoTIM (C), and monoTIM-K13A (D) in the presence (●) and absence (○) of 1 mM 2PG. Curves were obtained by monitoring the change in the CD signal at 222 nm.

**Table 3.** Kinetic parameters of the monoTIM active site variants<sup>a</sup>

Protein	$k_{cat}$ <sup>b</sup> (min <sup>-1</sup> )	$K_m$ <sup>b</sup> (mM)	$K_I$ (2PG) <sup>b</sup> (mM)
monoTIM	3.1 10 <sup>2</sup>	4.1 ± 0.6	52 ± 7
monoTIM-K13R	9.5	2.3 ± 0.3	66 ± 5
monoTIM-K13A	ND <sup>c</sup>	ND	ND
monoTIM-H95A	5.9	3.8 ± 0.8	334 ± 94
monoTIM-W-E97A	2.2 10 <sup>2</sup>	3.7 ± 0.6	28 ± 3

<sup>a</sup> The  $K_I$ 's have been calculated with GraFit, assuming competitive inhibition.

<sup>b</sup> With GAP as substrate.

<sup>c</sup> ND, not detectable.

$\chi_A$  has been decreased by 50° and  $\chi_C$  has been increased by 50°. As a net result, O-8 points further down than in the wild type (Fig. 7).

There are larger differences for the mode of binding of PGH, which is apparent from the dihedrals listed in Table 5. It shows that  $\chi_A$  has been reduced by 140° and  $\chi_C$  has been increased by 205°. The net result is also that O-8 points further down (Fig. 7). In this complex, there is no strong interaction between O-8(PGH) and N<sub>ε</sub>(Lys 13), because the side chain of Lys 13 is disordered (Borchert et al., 1995). The other interactions between polar atoms are similar; for example, O-8 and O-10 can form hydrogen bonds to N<sub>ε</sub>2(His 95), and N-9 interacts with O<sub>ε</sub>2(Glu 167) in both complexes.

In the monoTIM-W(2PG) complex, Lys 13 is well defined (Fig. 8A). Lys 13 is not involved in crystal contacts. The N<sub>ε</sub>(Lys 13) forms a hydrogen bond with O-8(2PG). This is also

observed in the wild type; nevertheless, the N<sub>ε</sub>(Lys 13) does have different interactions in this complex than in the wild type, because in the wild type, N<sub>ε</sub>(Lys 13) is salt bridged to Glu 97 of loop 4. This salt bridge is absent in the monoTIM-W(2PG) complex, as indicated in Figure 8A. Instead, Glu 97 is involved in a crystal-contact hydrogen-bonding network. This Lys 13-Glu 97 salt bridge is also absent in the monoTIM-SS(PGH) complex, as shown in Figure 8B. In this complex, Lys 13 is disordered, and Glu 97 is not involved in crystal contacts, but forms a salt bridge with His 95.

## Discussion

### Binding of the phosphate moiety of the inhibitors

The mode of binding of PGH and 2PG in the active site of monoTIM has been analyzed. As is shown in Figure 7 and Table 4, the phosphate moieties bind in the same way in monoTIM and the wild type. The polar phosphate oxygen atoms interact with main-chain atoms of loops 6, 7, and 8. These interactions keep the phosphate moiety rigidly in place, in monoTIM as well as in wtTIM, whereas in the triose part of the ligand molecule, the catalytic conversion takes place (Fig. 1). These tight interactions of the phosphate oxygen atoms are an important factor in preventing the methylglyoxal synthase side reaction. This side reaction does not occur in wild-type TIM, but it does occur in a variant in which loop 6 has been shortened by four residues (Pompliano et al., 1990). For monoTIM, there is no indication for enzyme-catalyzed formation of methylglyoxal. This agrees with the structural analysis showing that loop 6 of monoTIM also fixes the phosphate moiety in the same position and in the same way as in the wild type (Fig. 7).

**Table 4.** Contacts between the polar atoms of the ligand and the protein<sup>a</sup>

Atom	Contact distances between polar atoms			
Ligand atom	PGH in chicken TIM (wtTIM numbering)	PGH in monoTIM-SS	2PG in monoTIM-W	2PG in yeast TIM (wtTIM numbering)
O-1	N(Gly 235) 3.0	N(Gly 235) 3.0	N(Gly 235) 3.3	N(Gly 235) 3.3
O-2	N(Gly 173) 2.7 N(Ser 213) 2.8	O <sub>γ</sub> (Ser 213) 3.4 N(Ser 213) 2.5 N(Gly 173) 2.7	O(Ala171) 3.5 N(Gly 173) 2.8 N(Ser 213) 2.7 O <sub>γ</sub> (Ser 213) 3.3	O(Ala171) 3.4 N(Gly 173) 2.6 N(Ser 213) 2.7
O-3	N(Gly 234) 3.0	N(Gly 234) 2.9	N(Gly 234) 2.9	N(Ser 213) 3.1 N(Ala214) 3.4 N(Gly 234) 3.6
O-5	N <sub>ε</sub> (Lys 13) 3.4			N(Gly 234) 3.5
O-8	N <sub>ε</sub> (Lys 13) 2.8 N <sub>ε</sub> 2(His 95) 2.8	N <sub>δ</sub> 2(Asn 11) 2.5 N <sub>ε</sub> 2(His 95) 3.2	N <sub>δ</sub> 2(Asn 11) 3.2 N <sub>ε</sub> (Lys 13) 2.8 N <sub>ε</sub> 2(His 95) 3.2	N <sub>δ</sub> 2(Asn 11) 3.2 N <sub>ε</sub> (Lys 13) 3.2 N <sub>ε</sub> 2(His 95) 2.9
N-9/O-9	O <sub>ε</sub> 1(Glu 167) 3.1 O <sub>ε</sub> 2(Glu 167) 2.6	N <sub>ε</sub> 2(His 95) 3.2 O <sub>ε</sub> 2(Glu 167) 2.8	N <sub>ε</sub> 2(His 95) 3.1 O <sub>ε</sub> 1(Glu 167) 3.4 O <sub>ε</sub> 2(Glu 167) 2.6	N <sub>ε</sub> 2(His 95) 3.1 O <sub>ε</sub> 1(Glu 167) 3.3 O <sub>ε</sub> 2(Glu 167) 2.8
O-10	N <sub>ε</sub> 2(His 95) 3.0 O <sub>ε</sub> 1(Glu 167) 2.6 O <sub>ε</sub> 2(Glu 167) 2.9 N <sub>δ</sub> 2(Asn 11) 3.4	N <sub>ε</sub> 2(His 95) 2.4 O <sub>ε</sub> 1(Glu 167) 2.6 O <sub>ε</sub> 2(Glu 167) 2.4		

<sup>a</sup> All distances are in Å. N-9 and O-9 refer to PGH and 2PG, respectively (Fig. 3).

**Table 5.** Dihedrals of 2PG and PGH<sup>a</sup>

Dihedral	Atoms involved	PGH in chicken TIM	PGH in monoTIM-SS	2PG in monoTIM-W	2PG in yeast TIM
$\chi_a$	O-1-P-4-O-5-C-6	168.9	28.5	109.1	160.5
$\chi_b$	P-4-O-5-C-6-C-7	185.2	159.4	187.0	166.7
$\chi_c$	O-5-C-6-C-7-N-9/O-9	145.7	351.9	235.8	172.7
$\chi_d$	C-6-C-7-N-9/O-9-O-10	177.1	183.4		

<sup>a</sup> All angles are in degrees.  $\chi_d$  is close to 180°, in agreement with the cis geometry of the hydroxamate moiety. N-9 and O-9 refer to PGH and 2PG, respectively (Fig. 3).

It has been argued that the undesired methylglyoxal synthase side reaction (Richard, 1984) is also disfavored when the bridging oxygen atom (O-5) is in the same plane as the enediolate plane (minimizing orbital overlap between the enediolate  $\pi$  system and the C-6-O-5 bond [Lolis & Petsko, 1990]), which means that  $\chi_c$  (Table 5) should be 0° or 180° to optimally stabilize the enediolate intermediate. This is observed in the wild-type TIM complexes of 2PG and PGH, with  $\chi_c$  reasonably close to 180°, and also in the monoTIM-SS(PGH) complex, with  $\chi_c$  close to 0°, but not in the monoTIM-W(2PG) complex, with  $\chi_c$  = 236°. The mode of binding of PGH, which is the best analogue of the enediolate intermediate of the catalytic cycle, is in agreement with the absence of methylglyoxal synthase activity of monoTIM.

#### Catalytic glutamate

The first residue of loop 6 is the catalytic glutamate, Glu 167. The Glu 167 side chain is in a “swung-out” position in the unliganded form (Noble et al., 1993), interacting with Ser 96. In the presence of a ligand, this side chain adopts a “swung-in” conformation, interacting with the active site ligand. In monoTIM as well, as shown in Figure 7, Glu 167 adopts the “swung-in” conformation in the presence of a substrate analogue. In wild-type TIM, the loop-6 closure in the presence of ligand seems to be important for fixing the phosphate moiety into a rigid posi-

tion (Lolis & Petsko, 1990), as well as for facilitating the conformational switch of the Glu 167 side chain (Noble et al., 1993), and both these features are retained in monoTIM.

#### Catalytic lysine

Despite the increased conformational flexibility of loop 1, the mutagenesis studies prove that Lys 13 is essential for catalysis by monoTIM, because monoTIM-K13A is completely inactive. This is in agreement with observations with yeast TIM, where it was found that the yeast TIM-K13M variant was completely inactive (Lodi et al., 1994). However, for this mutant, the absence of activity was caused by the lack of binding of the substrate. The CD melting curves of monoTIM-K13A in the absence and presence of 1 mM 2PG show that 2PG still binds to monoTIM-K13A, indicating that substrate will bind to the active site of monoTIM-K13A. Nevertheless, monoTIM-K13A is inactive, suggesting that Lys 13 is essential for catalysis, as predicted by computer simulation (Bash et al., 1991). However, it is possible that in monoTIM-K13A, 2PG and substrate bind only with the phosphate moiety (in a nonproductive mode), and, therefore, binding cannot be detected by enzymatic assays. Electrostatic calculations with yeast TIM-K13M show that the reduced affinity of this active site for substrate and substrate analogues correlates with the presence of a much more negative

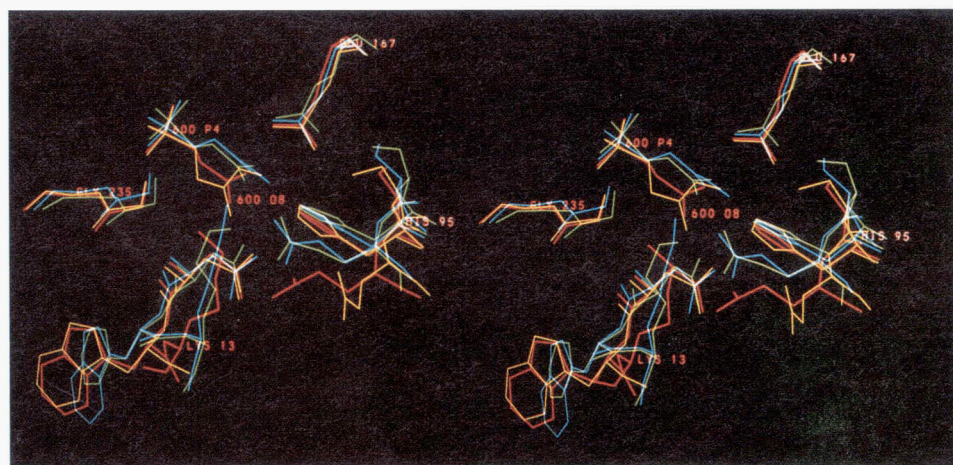


**Fig. 7.** Superposition of the active site geometries of four different structures: PGH bound to chicken TIM (blue), 2PG bound to yeast TIM (green), PGH bound to monoTIM-SS (yellow), and 2PG bound to monoTIM-W (red). Protein fragments shown are from loop 1 (with Lys 13), loop 4 (with His 95), loop 6 (with Glu 167), and loop 8 (with Gly 235).

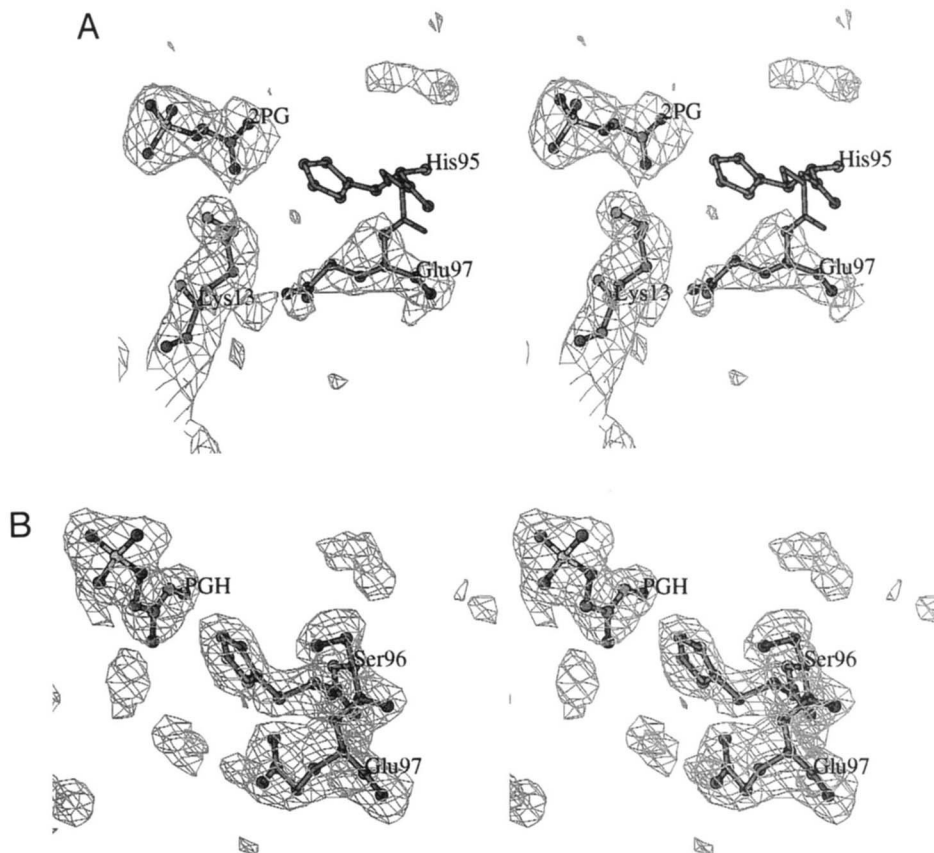


**Fig. 8.** Omit maps calculated after omit refinement. These maps were calculated with all data available between 30 Å and 2.4 Å. The contour level is 2.5 times the RMS deviation from the mean. **A:** Calculated from the monoTIM-W(2PG) structure, after omitting Lys 13, Glu 97, and 2PG. **B:** Calculated from the monoTIM-SS(PGH) structure, after omitting His 95-Ser 96-Glu 97 and PGH.

electrostatic potential, probably due to the presence of the uncompensated charge of the Glu 97 side chain (Joseph-McCarthy et al., 1994). This side chain adopts rather different conformations in the monoTIM structures. Glu 97 is a completely conserved glutamate in more than 30 TIM sequences, suggesting that its interactions are important for the function of TIM. In the wild type, it is held in position by a hydrogen bond with the side chain of Thr 75 of the other subunit, by van der Waals contacts with other atoms of the other subunit, and by a salt bridge with Lys 13 of the same subunit. However, in monoTIM, the Glu 97 side chain is seen in several different positions, none of them the same as in the wild type, and therefore the active site electrostatic potential will be very different. Even in the monoTIM-W(2PG) structure, no salt bridge is observed between Lys 13 and Glu 97, despite the fact that the Lys 13 is well ordered (Fig. 8A). Apparently, the Glu 97-Lys 13 salt bridge does not form in monoTIM. In agreement with this is the observation that monoTIM-W-E97A is as active as monoTIM itself (Table 3). In the monoTIM-W(2PG) structure, the Glu 97 side chain has adopted a conformation that is impossible in the wild-type dimer owing to severe clashes with atoms of loop 3 of the other subunit. Likewise, in the wild-type enzyme, loop 3 stabilizes the wild-type Lys 13 conformation via main-chain-main-chain hydrogen bonds and van der Waals contacts. Apparently, the

presence of loop 3 of the other subunit imposes the observed conformations of Lys 13 and Glu 97.

#### Catalytic histidine

The catalytic role of the histidine side chain is to facilitate the proton transfer between O-8 and O-10. As an intermediate in the proton transfer, a negatively charged imidazolate has been proposed (Lodi & Knowles, 1991). For this purpose, the histidine side chain is kept in place via a hydrogen bond between the unprotonated N<sub>δ</sub>1 and the peptide NH group of residue Glu 97. In the liganded monoTIM structures, the histidine side chain is correctly positioned, but not exactly in the same place as in the wild type (Fig. 7). The hydrogen bond between N<sub>δ</sub>1(His 95) and N(Glu 97) is weaker in the monoTIM structures. The structure of the main-chain trace of loop 4 near Glu 97 is also more variable in the monoTIM structures (Fig. 7), probably owing to the absence of the stabilizing interactions of the other subunit, present in the wild type. In monoTIM-SS(PGH), the environment of the histidine side chain is certainly different from that in the wild type, because here a salt bridge is observed between N<sub>δ</sub>1(His 95) and the side chain of Glu 97 (Fig. 8B). This salt bridge is not observed in monoTIM-W(2PG) (Fig. 8A). Apparently, in the monoTIM-SS(PGH) complex, the His 95 side chain

is doubly protonated, which is in disagreement with its catalytic role. Nevertheless, the variant monoTIM-H95A is still active, but 50 times less so than monoTIM, which proves that His 95 is important for optimal catalysis by monoTIM. In wild-type yeast TIM, His 95 has been changed into a glutamine (Nickbarg et al., 1988), and this variant also shows residual catalytic activity, as in monoTIM-H95A. This was explained by a change in mechanism: in yeast TIM-H95Q, all the proton transfer steps are now mediated by the side chain of the catalytic glutamate.

#### Mode of binding of the triose moiety of the inhibitors

The affinity of the active sites of monoTIM and wtTIM for 2PG differs only by a factor of two, as tabulated in Table 2, despite the fact that the mode of binding is somewhat different. In particular, the properties of the interacting Lys 13 are different. Nevertheless, the salt bridge between O-8(2PG) and N<sub>ε</sub>(Lys 13) in the monoTIM-W(2PG) complex seems to be important for the stability of the monoTIM-inhibitor complex. This interaction is missing in the monoTIM-SS(PGH) complex, owing to the disorder of the Lys 13 side chain, which correlates with a much weaker binding constant of PGH for the monoTIM active site. His 95 is clearly important for the binding of 2PG, because monoTIM-H95A has a sixfold lower affinity for 2PG. This is consistent with the presence of hydrogen bonds between O-8(2PG) and O-9(2PG) with N<sub>ε</sub>2(His 95). The mutation of His 95 into glutamine in yeast TIM also causes an eightfold reduction in the affinity for the inhibitor 2PG, whereas the  $K_m$  values for substrate are not much affected (Nickbarg et al., 1988), as in monoTIM-H95A.

Although the phosphate moieties of PGH and 2PG bind in the same way as in wild-type TIM, the triose parts adopt different conformations (Fig. 7; Table 5). The changed conformations of 2PG and PGH result in a further downward shift in the position of the O-8 atom (Fig. 7). This position is not possible in wild-type TIM because of clashes with the side chain of Lys 13. For example, after the superposition, the distance between O-8(2PG) in monoTIM and C<sub>ε</sub>(Lys 13) in wtTIM is 1.9 Å, and the distance between O-8(PGH) in monoTIM and C<sub>ε</sub>(Lys 13) in wtTIM is 2.3 Å. In wild-type TIM, the Lys 13 side chain has adopted, owing to subunit-subunit interactions, a position closer to the active site pocket, such that it does form a salt bridge with Glu 97. In wtTIM, atoms of Lys 13 and Glu 97 have, respectively, 5 and 15 contacts (within 4 Å) with atoms of the other subunit. For Cys 14, following immediately after Lys 13, there are 26 such intersubunit contacts (see also Fig. 5). These interactions much reduce the solvent accessibility of Lys 13 and Glu 97 and force the ( $\phi$ ,  $\psi$ ) of Lys 13 to become unfavorable in the wild type ( $\phi = 51^\circ$ ,  $\psi = -143^\circ$ ), whereas in monoTIM-W(2PG),  $\phi$  (Lys 13) = -86° [ $\psi$  (Lys 13) is undefined owing to the disorder of the next residues]. Apparently, in wild-type TIM, the second subunit fixes the active site residues of loop 1 and loop 4 of the first subunit in a rigid but strained conformation that is required for optimal catalysis. The second subunit also shields the active site pocket from the bulk solvent.

The mutational and structural data show that, in monoTIM, the same catalytic residues as in wild-type TIM are crucial for optimal catalysis. The binding of the high-affinity inhibitor 2PG induces the catalytic residues to adopt positions similar to those in the wild type. This suggests that the reaction mechanism of monoTIM will be the same as in wild type, although the cata-

lytic rate is much lower. This much lower rate is correlated with a different environment, such as an increased solvent accessibility, as well as a higher mobility of the catalytic lysine and histidine, due to the absence of the second subunit.

#### Materials and methods

##### DNA methods

Site-directed mutagenesis was performed by PCR using the overlap-extension procedure (Higuchi, 1990). The expression plasmid pET3a containing the monoTIM gene (Borchert et al., 1993b) was used as a template, except for the E97A mutation, which was introduced into the gene of monoTIM-W. The mutagenic PCR primers contain the following altered codons: A100W (GCA to TGG), F45S V46S (TTT GTT to TCG AGC), K13A (AAG to GCG), K13R (AAG to AGG), H95A (CAC to GCC), and E97A (GAG to GCA). DNA fragments carrying the point mutations were subcloned into the monoTIM-containing plasmid. The complete DNA sequence for all point-mutation monoTIM variants has been verified by using double-strand sequencing with the sequence kit (USB). *Escherichia coli* strain XL1-Blue (Bullock et al., 1987) was used as the host strain for the genetic manipulations.

##### Protein expression and purification

Expression of wtTIM (Borchert et al., 1993b), monoTIM (Borchert et al., 1994), and all its point mutation variants was carried out in *E. coli* strain BL21(DE3) (Studier & Moffatt, 1986). The transformants were grown in M9 medium with 100 mg/mL ampicillin. Cells were induced in the mid-log phase with 0.4 mM isopropyl-1-thio-β-D-galactoside and grown for another 8–14 h at a temperature of 18 °C.

Cells were lysed in two passages with a French press in 100 mM TEA, pH 8.0, 1 mM DTT, 1 mM EDTA, 1 mM azide. After 45–65% ammonium sulfate precipitation, protein was resuspended in 20 mM TEA, pH 8.0, 1 mM DTT, 1 mM EDTA, 1 mM azide, and 20 mM NaCl, and dialyzed overnight against the same buffer. The dialysate was loaded on an SP-Sepharose column calibrated with the same buffer and eluted with a 20–120 mM NaCl gradient. Because the binding properties of monoTIM-K13A are different, the loading buffer used for the purification of this variant did not contain NaCl, and the gradient was from 0 to 100 mM NaCl. The purity of all monoTIM variants was checked by SDS/PAGE analysis. Protein concentrations were determined with Bradford reagent using bovine serum albumin as a standard. The typical yield was between 10 and 20 mg of pure protein from 1 L of culture.

##### Enzyme assays

Standard assays for the conversion of the triose phosphates in both directions were carried out at 25 °C as described previously (Lambeir et al., 1987). It has been shown before that the ionic strength can affect the kinetics of trypanosomal TIM (Lambeir et al., 1987). Therefore, the NaCl concentration in the assay was kept constant within each set of experiments and always lower than 5 mM NaCl. The reaction was started by adding enzyme, and the change of absorbance at 340 nm was followed with a Lambda 2 spectrophotometer (Perkin-Elmer). The values of

$K_m$  and  $k_{cat}$  were determined with various amounts of substrate (0.5–10 mM GAP and 0.5–20 mM DHAP, respectively) and a fixed protein concentration. For the determination of the  $K_f$  of the conversion of GAP into DHAP, this procedure was repeated several times at various concentrations of the inhibitors. For the calculation of kinetic parameters and error estimates, the programs UltraFit (Biosoft, Cambridge, U.K.) and GraFit (Leatherbarrow, 1992) were used. The formation of methylglyoxal was measured according to Gawehn and Bergmeyer (1974).

PGH was synthesized from tri(monocyclohexylammonium) 2-phosphoglycolate (Sigma-Aldrich Chemie GmbH, Germany), which was first converted into the free acid form using Dowex 50W-H<sup>+</sup>. Treatment of the 2-phosphoglycolic acid with 2,2-dimethoxypropane in methanol yielded the methyl ester of 2PG, which was converted to PGH (Collins, 1974). Purification of PGH to homogeneity was done on a DEAE Sephadex A-25 column using a 0–0.4 M lithium chloride gradient. Two consecutive purification columns were needed to obtain a product free of 2PG. PGH was isolated from LiCl by precipitation with barium salts (Lewis & Lowe, 1977). The purity of the barium salt of PGH was confirmed by <sup>31</sup>P NMR and <sup>1</sup>H NMR and mass spectrometry. PGH solutions were prepared as described (Lewis & Lowe, 1977), and the concentration of dissolved PGH was determined spectrophotometrically (Collins, 1974).

### Thermal stability

CD spectra at different temperatures were recorded on a Jasco J-710 spectropolarimeter. Temperature denaturation studies in the presence and absence of 1 mM 2PG were carried out by monitoring the ellipticity at 222 nm at increasing temperatures from 20 to 70 °C, with a scan rate of 20 °C per hour. Cuvettes with a 0.2-cm path length were used. The protein solution (0.4 mg/mL) was in a 20 mM MOPS buffer, pH 7.0, containing also 1 mM DTT, 1 mM EDTA, and 1 mM azide. For all samples, it was observed that the denaturation is irreversible.

### Structure analysis

The crystal structures of monoTIM (Borchert et al., 1993a), monoTIM-SS, monoTIM-SS(PGH), and monoTIM-W(2PG) (Borchert et al., 1995) have been refined at a maximum resolution of 2.4 Å. The crystal structures (Table 1) have been analyzed with the O package (Jones et al., 1991) and the WHAT IF program (Vriend, 1990). For the comparison, the structures of chicken TIM(PGH), refined at 1.7 Å resolution (Davenport et al., 1991), and of yeast TIM(2PG), refined at 2.5 Å resolution (Lolis & Petsko, 1990), were used; the PDB entry codes of these structures are 1TPH and 2YPI, respectively. The PDB entry code of the structure of wtTIM, refined at 1.83 Å resolution (Wierenga et al., 1991), is 5TIM. All superpositions were calculated with the C<sub>α</sub> atoms of the framework β strands and α helices.

### Acknowledgments

This research was supported by EC grant BIOT-CT90-0182. We thank Dr. Abagyan (Skirball Institute, New York) for his help with ICM, and Drs. Reinstein (MPI, Dortmund), Larsen (EMBL, Grenoble), and Schloss (University of Kansas) for useful discussions.

### References

- Abagyan RA, Totrov MM, Kuznetsov DN. 1994. ICM – A new method for protein modelling and design: Applications to docking and structure prediction from the distorted native conformation. *J Comput Chem* 15:488–506.
- Bash PA, Field MJ, Davenport RC, Petsko GA, Ringe D, Karplus M. 1991. Computer simulation and analysis of the reaction pathway of triosephosphate isomerase. *Biochemistry* 30:5826–5832.
- Blacklow SC, Knowles JR. 1990. How can a catalytic lesion be offset? The energetics of two pseudorevertant triosephosphate isomerases. *Biochemistry* 29:4099–4108.
- Borchert TV, Abagyan R, Jaenicke R, Wierenga RK. 1994. Design, creation, and characterization of a stable, monomeric triosephosphate isomerase. *Proc Natl Acad Sci USA* 91:1515–1518.
- Borchert TV, Abagyan R, Radha Kishan KV, Zeelen JP, Wierenga RK. 1993a. The crystal structure of an engineered monomeric triosephosphate isomerase, mono TIM: The correct modelling of an eight-residue loop. *Structure* 1:205–213.
- Borchert TV, Kishan KR, Zeelen JP, Schliebs W, Thanki N, Abagyan R, Jaenicke R, Wierenga RK. 1995. Three new structures of point mutation variants of monoTIM: Conformational flexibility of loop 1, loop 4 and loop 8. *Structure* 3:669–679.
- Borchert TV, Pratt K, Zeelen JP, Callens M, Noble MEM, Opperdoes FR, Michels PAM, Wierenga RK. 1993b. Over-expression of trypanosomal triosephosphate isomerase in *Escherichia coli* and characterisation of a dimer-interface mutant. *Eur J Biochem* 211:703–710.
- Bullock WO, Fernandez JM, Short JM. 1987. XL1-blue: A high efficiency plasmid transforming recA *Escherichia coli* strain with B-galactosidase selection. *BioTechniques* 5:376–378.
- Collins KD. 1974. An activated intermediate analogue. The use of phosphoglycolohydroxamate as a stable analogue of a transiently occurring dihydroxyacetone phosphate-derived enolate in enzymatic catalysis. *J Biol Chem* 249:136–142.
- Davenport RC, Bash PA, Seaton BA, Karplus M, Petsko GA, Ringe D. 1991. Structure of the triosephosphate isomerase-phosphoglycolohydroxamate complex: An analogue of the intermediate on the reaction pathway. *Biochemistry* 30:5821–5826.
- Gawehn K, Bergmeyer HU. 1974. Methylglyoxal. In: Bergmeyer HU, ed. *Methoden der enzymatischen Analyse*. Weinheim, Germany: Verlag Chemie GmbH. pp 1542–1544.
- Higuchi R. 1990. Recombinant PCR. In: Innis MA, Gelford DH, Sninsky JJ, White TJ, eds. *PCR protocols: A guide to methods and applications*. San Diego, California: Academic Press. pp 177–183.
- Jones TA, Zou JY, Cowan SW, Kjeldgaard M. 1991. Improved methods for building protein models in electron density maps and the location of errors in these models. *Acta Crystallogr A* 47:110–119.
- Joseph D, Petsko GA, Karplus M. 1990. Anatomy of a conformational change: Hinged “lid” motion of the triosephosphate isomerase loop. *Science* 249:1425–1428.
- Joseph-McCarthy D, Lolis E, Komives EA, Petsko GA. 1994. Crystal structure of the K12M/G15A triosephosphate isomerase double mutant and electrostatic analysis of the active site. *Biochemistry* 33:2815–2823.
- Knowles JR. 1991. Enzyme catalysis: Not different, just better. *Nature* 350:121–124.
- Knowles JR, Albery WJ. 1977. Perfection in enzyme catalysis: The energetics of triosephosphate isomerase. *Acc Chem Res* 10:105–111.
- Lambeir AM, Opperdoes FR, Wierenga RK. 1987. Kinetic properties of triosephosphate isomerase from *Trypanosoma brucei brucei*. A comparison with the rabbit muscle and yeast enzymes. *Eur J Biochem* 168:69–74.
- Leatherbarrow RJ. 1992. *GraFit*. Staines, UK: Erithacus Software Ltd.
- Lewis DJ, Lowe G. 1977. Inhibition of fructose-1,6-biphosphate aldolase from rabbit muscle and *Bacillus stearothermophilus*. *Eur J Biochem* 80:119–133.
- Lodi PJ, Chang LC, Knowles JR, Komives EA. 1994. Triosephosphate isomerase requires a positively charged active site: The role of lysine-12. *Biochemistry* 33:2809–2814.
- Lodi PJ, Knowles JR. 1991. Neutral imidazole is the electrophile in the reaction catalyzed by triosephosphate isomerase: Structural origins and catalytic implications. *Biochemistry* 30:6948–6956.
- Lolis E, Petsko GA. 1990. Crystallographic analysis of the complex between triosephosphate isomerase and 2-phosphoglycolate at 2.5-Å resolution: Implications for catalysis. *Biochemistry* 29:6619–6625.
- Nickbarg EB, Davenport RC, Petsko GA, Knowles JR. 1988. Triosephosphate isomerase: Removal of a putatively electrophilic histidine residue results in a subtle change in catalytic mechanism. *Biochemistry* 27:5948–5960.
- Noble MEM, Zeelen JP, Wierenga RK. 1993. Structures of the “open” and “closed” state of trypanosomal triosephosphate isomerase, as observed

- in a new crystal form: Implications for the reaction mechanism. *Proteins Struct Funct Genet* 16:311–326.
- Pompliano DL, Peyman A, Knowles JR. 1990. Stabilization of a reaction intermediate as a catalytic device: Definition of the functional role of the flexible loop in triosephosphate isomerase. *Biochemistry* 29:3186–3194.
- Richard JP. 1984. Acid-base catalysis of the elimination and isomerization reactions of triose phosphates. *J Am Chem Soc* 106:4926–4936.
- Studier FW, Moffatt BA. 1986. Use of the bacteriophage T7 RNA polymerase to direct selective high-level expression of cloned genes. *J Mol Biol* 189:113–130.
- Vriend G. 1990. WHAT IF: A molecular modelling and drug design program. *J Mol Graph* 8:52–56.
- Waley SG. 1973. Refolding of triose phosphate isomerase. *Biochem J* 135: 165–172.
- Wierenga RK, Borcherdt TV, Noble MEM. 1992. Crystallographic binding studies with triosephosphate isomerase: Conformational changes induced by substrate and substrate-analogues. *FEBS Lett* 307:34–49.
- Wierenga RK, Noble MEM, Vriend G, Nauche S, Hol WGJ. 1991. Refined 1.83 Å structure of trypanosomal triosephosphate isomerase crystallized in the presence of 2.4 M ammonium sulphate. A comparison with the structure of the trypanosomal triosephosphate isomerase-glycerol-3-phosphate complex. *J Mol Biol* 220:995–1015.
- Williams JC, McDermott AE. 1995. Dynamics of the flexible loop of triosephosphate isomerase: The loop motion is not ligand gated. *Biochemistry* 34:8309–8319.
- Wolfenden R. 1969. Transition state analogues for enzyme catalysis. *Nature* 223:704–705.
- Zabori S, Rudolph R, Jaenicke R. 1980. Folding and association of triose phosphate isomerase from rabbit muscle. *Z Naturforsch* 35C:999–1004.